omitting the $R(39°)$ is shown in the first line of Table IV. Comparing to the line below it for the full data set, it is obvious that most of the phases are very sensitive to this datum, both in their values and standard deviations. Such a situation is rather undesirable: One would prefer that the results not depend on a single datum.

V. DETAILED FIT TO THE DATA

The experimental data and the corresponding predictions are displayed in Table VI and Figs. 1–3.

The too-good fit of the relative cross-section data, Fig. 1, is presumably accidental. The $\sigma(90°)$ prediction is within both of the experimental errors, so it is in agreement with both measurements. Removal of either or both of the Minnesota $\sigma(90°)$ and Rutherford $P(45°)$ data had no significant effect on the analyses.

ACKNOWLEDGMENTS

The author is much indebted to N. R. Yoder for helpful discussion and to J. Litt for communication of data in advance of publication. The computations were performed in the Computation Center of the Michigan State University, with the assistance of M. D. Miller.

PHYSICAL REVIEW VOLUME 139, NUMBER 2B 26 JULY 1965

Analysis of Single Excitations in Inelastic Deuteron Scattering from Ni^{60}, Zr^{92}, and Sn^{120} Nuclei*

R. K. Jolly†
Department of Physics, University of Pittsburgh, Pittsburgh, Pennsylvania
(Received 2 November 1964; revised manuscript received 22 March 1965)

Inelastic scattering of 15-MeV deuterons from Ni^{60}, Zr^{92}, and Sn^{120} nuclei has been studied with adequate resolution to enable identification of almost all states of known spin and parity. Detailed angular distributions of deuteron groups corresponding to well-resolved states of these nuclei have been measured and compared with distorted-wave Born approximation calculations for single excitations using a deformed optical-model potential. The theoretical predictions, including Coulomb excitation and for a complex coupling, are found to be quite successful for strongly excited states. The status of the Blair phase rule is discussed in the context of the aforesaid comparison. Spin and parity assignments are made for several new levels. Excitation energies, differential cross sections, and reduced transition probabilities have been tabulated and compared with previously known values.

I. INTRODUCTION

In a previous paper[1] angular distributions of inelastically scattered deuterons from Ni were reported and the results along with those for Sn and Zr taken from an earlier work of Cohen and Price[2] were examined to check the validity of the Blair phase rule. Blair[3] has shown that, under certain approximations, the angular distribution of inelastically scattered particles is oscillatory, and for angles $\lesssim 60°$ the phase of these oscillations, relative to that of the oscillations in the angular distribution for the elastically scattered particles, depends on the angular momentum transferred in the inelastic process. The angular distributions for the inelastic groups are in or out of phase with that for the elastic group, depending on whether the angular momentum transferred is odd or even, respectively. This result, if true, offers a very convenient tool for parity assignments to nuclear levels, and therefore a detailed investigation of the validity of this rule was undertaken as reported in Ref. 1. The conclusions of the above study were that the phase rule holds for the strongly excited states and that there are important differences between the angular distributions for the strongly excited and weakly excited levels of the same parity. It was also noticed that members of the two-phonon triplet showed angular distributions somewhat like those of negative parity states. On account of its partial success, the phase rule was used for parity assignments only with caution.

However, recent theoretical and experimental work on inelastic scattering of α particles[4] and protons[5] has proved inelastic scattering to be a dependable tool for nuclear spectroscopy, particularly of the strongly excited states. Distorted-wave Born approximation (DWBA) calculations have successfully reproduced the angular distributions for single quadrupole and octupole oscillations using a nonspherical optical-model poten-

* Work supported by the National Science Foundation, the U. S. Office of Naval Research, and the U. S. Air Force Office of Scientific Research.

† Present address: Physics Department, Florida State University, Tallahassee.

[1] R. K. Jolly, E. K. Lin, and B. L. Cohen, Phys. Rev. **128**, 2292 (1962).

[2] B. L. Cohen and R. E. Price, Phys. Rev. **123**, 283 (1961).

[3] J. S. Blair, Phys. Rev. **118**, 928 (1959); also *Direct Interactions and Nuclear Reaction Mechanisms*, edited by E. Clemental (Gordon and Breach Science Publishers, New York, 1963).

[4] E. Rost, Phys. Rev. **128**, 2708 (1962).

[5] T. Stovall and N. M. Hintz, Phys. Rev. **135**, B330 (1964).

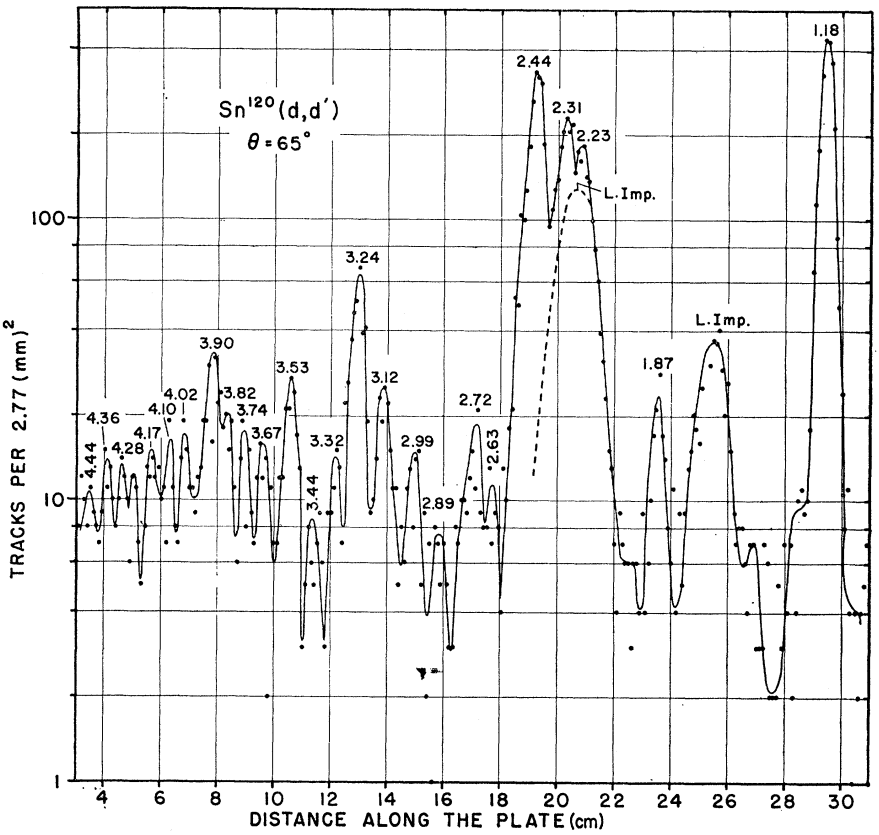

FIG. 1. Energy spectrum from inelastic scattering of deuterons from Sn^{120} taken with the magnetic spectrograph. The plot is intensity versus distance along the plate. The numbers that appear on the intensity peaks are the excitation energies of the states of the target nucleus measured from the ground state. θ is the scattering angle. Graphs marked L. Imp. are due to the presence of light contaminants in the target.

tial. The theoretical predictions have been most successful for α particles, and though intermediate-energy deuterons are not as strongly absorbed as α particles, one nevertheless expects a reasonable degree of success for inelastic-deuteron-scattering predictions. Consequently, relying on this hope, a detailed comparison between theory and experiment in an extended mass region ($A=60$–120) was undertaken. Ni^{60}, Zr^{92}, and Sn^{120} nuclei were chosen, since they had a great many levels of known spin and parity that could be easily resolved and had, in addition, several levels of the same spin and parity among which the angular distributions could be compared.

II. EXPERIMENT

A. $Sn^{120}(d,d')$

The intensity and angular distributions of deuteron groups from Sn^{120} were measured using the scattering facility of the University of Pittsburgh cyclotron laboratory. Details of this arrangement have been discussed elsewhere[2,6] but briefly, the scattered particles from the scattering chamber are analyzed in passing through a wedge-magnet spectrograph and detected on a nuclear emulsion plate placed at the focal plane of the magnetic spectrograph. The energy spectra are then obtained by counting the track densities along the plate under a microscope. Typical data are shown in Fig. 1. The average energy resolution is $\sim$65 keV. The groups marked L. Imp. are due to the elastically scattered deuterons from O^{16} and C^{12} impurities in the target, which was a self-supporting foil. For angular distributions the spectrograph could be turned about the axis of the scattering chamber from $-20°$ to $+140°$, although beyond 90° it required a time-consuming change of scattering chambers and the destruction of the scattering-chamber vacuum for every change of angle. The angular distributions for the states of Sn^{120} up to 4.8 MeV of excitation energy were measured from 20° to 90° with 5° intervals.

B. $Ni^{60}(d,d')$ and $Zr^{92}(d,d')$

These data were taken with a dE/dx-E solid-state detector system, although some spectra were also measured with a magnetic spectrograph which gave better energy resolution. The scattering system used was also different from the one described in the previous paragraph. Some details of this arrangement are given below, but more details can be found in Ref.s 7 and 8. The

[6] R. S. Bender, E. M. Reilley, A. J. Allen, R. Ely, J. S. Arthur, and H. J. Hausman, Rev. Sci. Instr. **23**, 542 (1952).

[7] C. D. Goodman and J. B. Ball, Phys. Rev. **118**, 1062 (1960); **120**, 488 (1960).

[8] R. H. Fulmer and W. W. Daehnick (to be published).

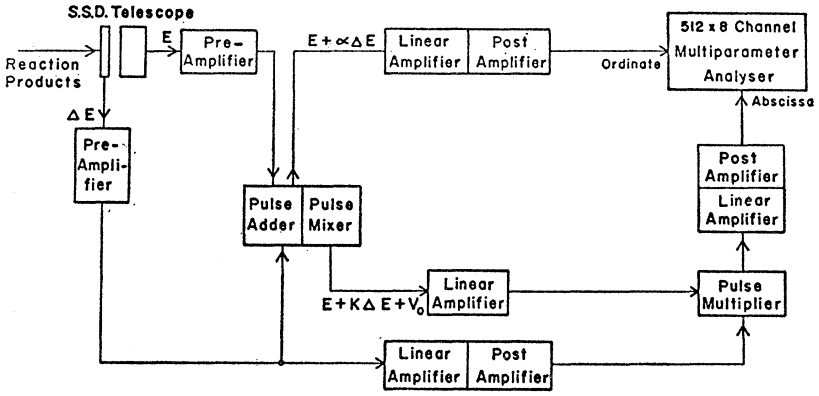

FIG. 2. A schematic block diagram of the electronics for the transmission (ΔE) and stopping (E) solid-state detector arrangement.

deuteron beam from the cyclotron, after focusing and preliminary energy analysis, passed into the magnetic spectrograph, since the latter was set at a scattering angle of zero degrees. The spectrograph was used for further energy analysis (and consequent suppression of scattering from edges of slits) of the incident beam, and at the appropriate field strength focused most of the beam at the center of its focal plane, whence the beam passed through a collimating arrangement of slits at the entrance to a scattering chamber, illuminated a target and was measured in a Faraday cup at the far end of the scattering chamber. The chamber has a motorized turntable that carries a telescopic arrangement of a transmission and a stopping solid-state detector. This new beam-handling arrangement was found to reduce both the beam intensity and background, although the former effect can be compensated for by decreasing the target-detector separation without much sacrifice in resolution. The pulses from the transmission (ΔE) and the stopping detector (E) were routed into an arrangement of preamplifiers, amplifiers, and adder, mixer, and multiplier circuits shown in a block diagram in Fig. 2. Finally, the "sum" and the "product" pulses were fed, respectively, into the ordinate and abscissa of a 4096-channel analyzer used in a multiparameter operation mode (typically 512×8).

Typical data for Ni^{60} and Zr^{92} nuclei, obtained with the scattering and measurement facility described above, are presented in Figs. 3 and 4, respectively. The energy resolution obtained in Ni spectra was typically ~70 keV, while in Zr spectra it was ~110 keV.

The light impurity groups that are seen to interfere with the 1.33- and 5.82-MeV groups in Fig. 3 originate from the ground and the first excited states of C^{12} impurity in the Ni^{60} target. The angular distributions at 5° intervals were measured from 25° to 110° for the states of Zr^{92} up to 4.5 MeV of excitation energy and from 25° to 157° for the states of Ni^{60} up to 6.2 MeV of excitation energy.

III. DWBA CALCULATIONS OF INELASTIC-SCATTERING CROSS SECTIONS

In DWBA calculations for vibrational excitations[9] in even-even nuclei ($J_i=0$, $J_f=l$), one deals with cross

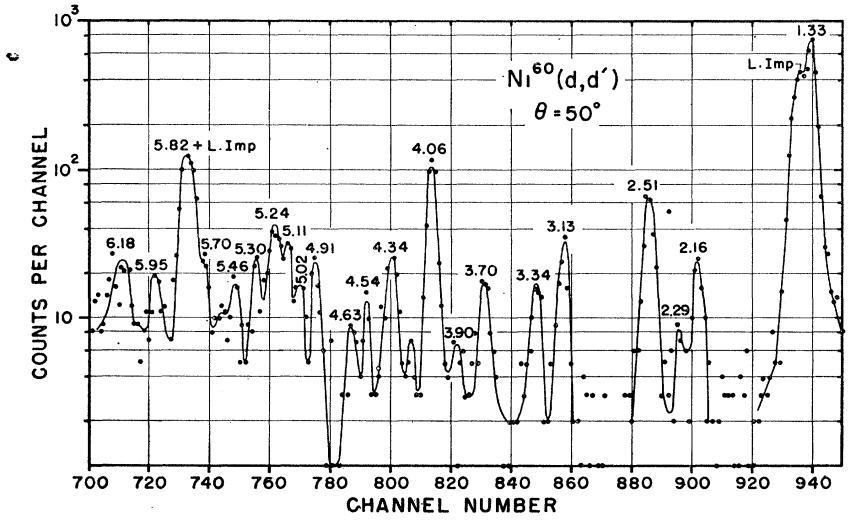

FIG. 3. Energy spectrum from inelastic scattering of deuterons from Ni^{60} taken with the ΔE-E system. The plot is of intensity versus channel number in the energy axis (ordinate) of the 4096-channel analyzer used in the multiparameter operation mode. See also the caption for Fig. 1.

[9] R. H. Bassel, R. M. Drisko, G. R. Satchler, and E. Rost, Phys. Rev. 128, 2693 (1962); G. R. Satchler, Nucl. Phys. 55, 1 (1964).

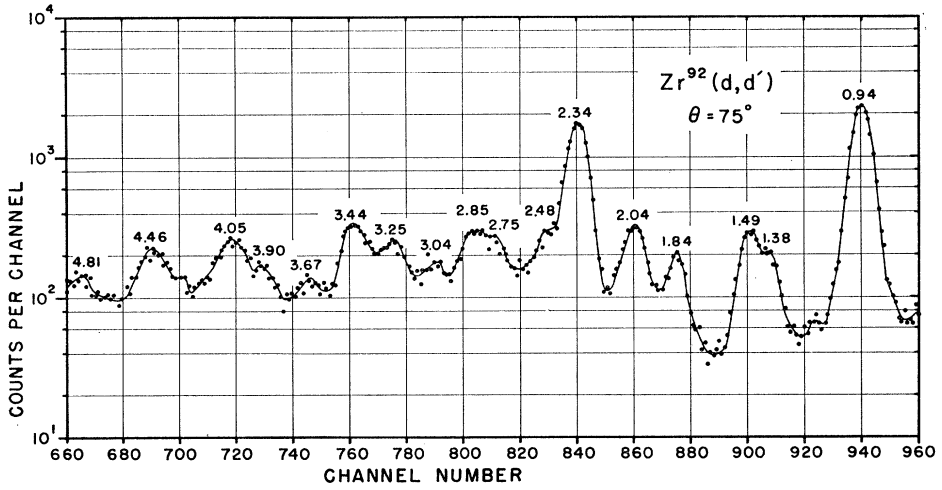

FIG. 4. Energy spectrum from inelastic scattering of deuterons from Zr^{92} taken with the ΔE-E system. See also the caption for Fig. 3.

sections of the form

$$(d\sigma/d\Omega)_l=\beta_l^2\sigma_l(\theta) \tag{1}$$

for inelastic scattering involving an angular-momentum transfer l to the nucleus. β_l^2 is the mean-square deformation of the vibrational state and is related to the corresponding reduced transition probability[10] by the formula

$$B(El;0\rightarrow l)=((3/4\pi)ZeR_0^l)^2\beta_l^2. \tag{2}$$

The $B(El)$'s are usually expressed in terms of single-particle estimates, for which the following relation may be used:

$$\frac{B(El;0\rightarrow l)}{B_{\text{s.p.}}(El;0\rightarrow l)}=\frac{(3+l)^2}{2l+1}\frac{Z^2}{4\pi}\beta_l^2. \tag{3}$$

Numerical values of β_l's and reduced transition probabilities for the various states investigated in this work are listed in Tables II, III, and IV.

The angle-dependent factor $\sigma(\theta)$ in (1) was calculated on an IBM-7090 computer using the Oak Ridge code JULIE.[11] The optical-potential parameters used (Table I) were the best-fit parameters of Perey and Perey[12] obtained from analysis of the elastic deuteron scattering data reported by Jolly *et al.* in an earlier paper.[13] The optical-model potential used in these analyses was of the form

$$U(r)=-V\left(\frac{1}{e^x+1}\right)-i\left(W-W'\frac{d}{dx'}\right)\left(\frac{1}{e^{x'}+1}\right)+\begin{cases}Ze^2/r & \text{for } r>R_c\\ Ze^2/2R_c(3-r^2/R_c^2) & \text{for } r\leqslant R_c,\end{cases} \tag{4}$$

where $x=(r-R)/a$, $R=r_0A^{1/3}$, and R_c is the Coulomb radius. The value $x=x'$ corresponds to values of the radius and diffuseness parameters, r_0' and a', respectively, for the imaginary part of the complex potential. The absorptive part of (4) has two strengths W and W' corresponding, respectively, to the volume and surface form factors. However, for 15-MeV deuterons, surface absorption is believed to be dominant, so that W was set equal to zero in the analyses of elastic-scattering data. There are two types of potentials listed in Table I (types "*a*" and "*b*"). The 100-MeV-deep potential is believed to be physical, as it is similar to the sum of the neutron and proton potentials and also gives reasonably correct spectroscopic factors for the states excited via (d,p) reactions. The optical-model fits to the elastic-scattering data for the 100-MeV-deep potential (type *b*) are shown in Fig. 5.

DWBA calculations of the inelastic-scattering cross section were made using the surface-coupling collective model.[9] While the model is a poor one for a simple shell-model state, the form factor is expected to be sufficiently similar to that obtained for single excitations (levels excited by a one-step process) to give a proper shape for the angular distribution but not necessarily a correct β_l. Calculations using this model were done using the same deuteron parameters for the entrance and exit

TABLE I. 15-MeV deuteron optical potential parameters (types "*a*" and "*b*" of Ref. 12) for the elements Ni^{58}, Zr, and Sn^{120}. See Fig. 5 for optical-model fits, using the potential type "*b*," to the elastic-deuteron-scattering angular distributions from these nuclei.

Element	Type	V (MeV)	r_0 (F)	a (F)	W' (MeV)	r_0' (F)	a' (F)	X^2
Ni^{58}	*a*	76.1	0.931	0.840	44.60	1.284	0.850	1.0
	b	98.6	1.105	0.709	65.96	1.170	0.831	1.1
Zr	*a*	68.1	1.098	0.911	46.64	1.404	0.682	0.63
	b	98.1	1.127	0.848	59.48	1.394	0.655	0.71
Sn^{120}	*a*	75.3	1.104	0.688	41.16	1.247	0.940	0.65
	b	99.7	1.168	0.611	48.56	1.213	0.985	0.83

[10] K. Alder, A. Bohr, T. Huus, B. Mottelson, and A. Winther, Rev. Mod. Phys. **28**, 432 (1956).
[11] R. M. Drisko, R. H. Bassel, and G. R. Satchler (unpublished).
[12] C. M. Perey and F. G. Perey, Phys. Rev. **132**, 755 (1963).
[13] R. K. Jolly, E. K. Lin, and B. L. Cohen, Phys. Rev. **130**, 2391 (1963).

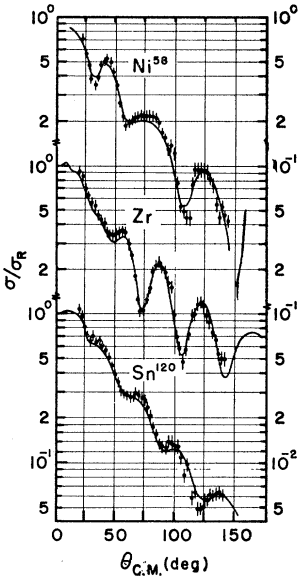

FIG. 5. Optical-model fits to the data from Ni^{58}, Zr, Sn^{120} obtained by Perey and Perey (Ref. 12) using potential type "*b*." (Table I.)

channels and also using both types of deuteron potential (*a* and *b*). In all cases, with the exception of large angles ($\gtrsim 90°$), angular distributions were found to be practically identical for the above two sets of parameters. Figure 6 shows a comparison of the angular distributions for the potential types "*a*" and "*b*" in the case of Zr^{92}. There seems to be an appreciable difference in magnitude for the $l=2$ case, but the shapes of the two angular distributions are essentially identical within experimental uncertainties and the validity of the surface-coupling model for single excitations.

Preliminary calculations were also done both with and without the contribution from Coulomb excitation. The principal effect of including Coulomb excitation was to decrease the peak-to-valley ratio of the angular distributions at forward angles. As we shall see in Figs. 8, 11, and 13, the agreement between single-excitation predictions and the experimental data is considerably improved, especially for the quadrupole states in heavier nuclei, as may be expected. Consequently, all analyses presented in this paper were done using calculations including Coulomb-excitation effects.

Calculations were also done with both real and complex coupling for single quadrupole and octupole excitations. A comparison of the two calculations with the experimental data for the strongly excited octupole and quadrupole states in Zr^{92} is shown in Fig. 7. The conclusion from the case of Zr^{92} is quite typical of the situation in the other two nuclei, i.e., both shapes and magnitudes of the single-excitation cross sections are predicted correctly by the complex-coupling calculations only. Consequently, all analyses of the data presented in this paper were done with calculations including complex coupling.

Calculations including the contribution from Coulomb excitation were done for all possible l and Q values, except $l=0$ where Coulomb excitation could not be included for the following reasons:

(1) The fifty partial waves allowed by code JULIE are not enough.

(2) $l=0$ Coulomb excitation would imply the excitation of a "breathing" mode, which is unlikely at these energies.

IV. ANALYSIS OF (*d*,*d'*) SPECTRA IN Sn^{120}, Zr^{92}, AND Ni^{60}

A. Excitation Energies

Energy spectra of inelastically scattered deuterons from Sn^{120}, Zr^{92}, and Ni^{60} nuclei have been measured using the technique described above. The results are

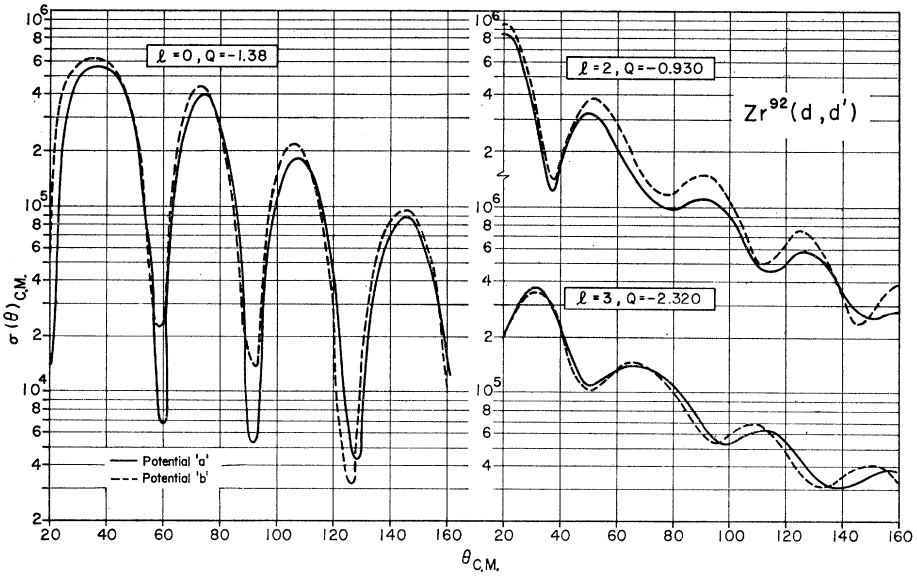

FIG. 6. A comparison of DWBA calculations (excluding Coulomb-excitation effects) of differential cross sections using potential types "*a*" and "*b*" (Table I) for Zr^{92} (*d*,*d'*) and for different l and Q values indicated in the figure.

listed in Tables II–IV. The excitation energies listed in these tables are the averages of measurements made at several angles. The uncertainties in the quoted values are ~5 keV per MeV of excitation energy, i.e., for example, ~20 keV for a state at 4 MeV of excitation energy.

B. Angular Distributions and Spectroscopic Analysis

Angular distributions of inelastically scattered deuterons from Sn^{120}, Zr^{92}, and Ni^{60} were measured by the methods described above. The results were compared with the DWBA predictions for single excitations described in the previous section. The shape agreement

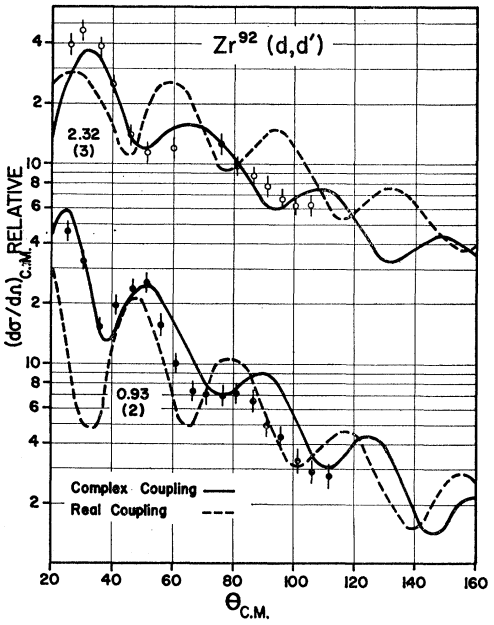

FIG. 7. A comparison between DWBA calculations and the experimental data for the strongly excited 2^+ and 3^- states in Zr^{92}. The solid curve is the DWBA calculation using complex coupling while the broken curve is the calculation using real coupling. The numbers without parentheses are excitation energies, while those within parentheses are the values of the angular-momentum transfer in the inelastic collision.

between theoretical and experimental angular distributions was found quite good in all known cases of single excitations, and the values of reduced transition strengths in terms of single-particle estimates, $B(El)/B_{s.p.}(El)$, agree fairly well with their values as known from other sources. It may be pointed out that the model used in the DWBA calculations discussed here is not expected to be valid for any level which can be reached by a two-or-more-step excitation, and as mentioned earlier, it may be somewhat in error for a one-step excitation process if the form factor differs drastically from that of the surface-coupling collective model. However, in both of these instances one expects weak excitations. With the aforesaid limitations of the

TABLE II. Spectroscopic data from inelastic scattering of 15-MeV deuterons from Sn^{120}. The spin and parity (J^π) assignments have been made on the basis of comparisons of experimental angular distributions and DWBA calculations. Details of calculating $B(El)/B_{s.p.}(El)$ and β_l are explained in the text.

Excitation energy (MeV)					$B(El;0\to l)/B_{s.p.}(El;0\to l)$			
			J^π			Elsewhere		
Present work	Ref. 16	$d\sigma/d\Omega(51°)_{c.m.}$ (mb/sr)	Present work	Ref. 16	Present work	Ref. 14	Ref. 17	β_l
1.18	1.18	1.26	2^+	2^+	15	11	13	0.12
1.87	1.89	0.035	(0^+)	0^+				
2.11		0.033						
2.23	2.22	0.09		4^+				
2.31		0.14						
2.44	2.42	0.78	3^-		20			0.14
2.63	2.62	0.032	$(0^+?)$	0^+				
2.72		0.051	(2^+)		0.8			0.03
2.89		0.037						
2.99		0.041						
3.12		0.055						
3.24		0.13						
3.32		0.031						
3.44		0.022						
3.53		0.073	(2^+)		1.3			0.04
3.67		0.053						
3.74		0.029						
3.82		0.044						
3.90		0.049						
4.02		0.029	(2^+)		0.6			0.03
4.10		0.025						
4.17		0.022						
4.28		0.023						
4.36		0.020						
4.44		0.030						
4.60		0.033						

DWBA calculations in mind, spin and parity assignments and calculations of reduced transition strengths and deformabilities β_l have been made for levels of unknown assignments, and the results have been listed in the Tables II–IV, and presented in Figs. 8–15 in this section. In Figs. 8, 11, and 13 the theoretical curves for the strongly excited 2^+ and 3^- levels have been presented for the calculations done both with and without the inclusion of Coulomb-excitation effects, to demonstrate that Coulomb-excitation effects are important at small angles and that the agreement with the experimental data is considerably improved by the inclusion of these effects in the theoretical calculations. Consequently, all comparisons of experimental data

TABLE III. Spectroscopic data from inelastic scattering of 15-MeV deuterons from Zr^{92}. See also the caption for Table II.

Excitation energy (MeV)							$B(El;0\to l)/B_{s.p.}(El;0\to l)$		
	Elsewhere			J^π	Elsewhere				
Present work	Ref. 16	Ref. 18	$d\sigma/d\Omega(50°)_{c.m.}$ (mb/sr)	Present work	Ref. 16	Ref. 18	Present work	Ref. 19	β_l
0.94	0.93	0.94	2.02	2^+	2^+	2	6	8	0.10
1.38	1.39	1.38	0.15	(0^+)	$0^{(+)}$	0			
1.49	1.50	1.50	0.15		4^+	4			
1.84	1.84	1.88	0.23		2^+	2			
2.04	2.05	2.07	0.17			2			
2.34	2.35		0.44	3^-	3^-		12		0.14
2.48			0.10						
2.75			0.03						
2.85			0.07						
3.04		3.06	0.08						
3.25			0.08						
3.44			0.10	(3^-)			3		0.07
3.67		3.69	0.03			1–4			
3.90			0.09						
4.05		4.03	0.18			(2,3,4)			
4.46			0.16						
4.81		4.80	0.10			(6)			
5.51		5.50	0.10			1–4			

TABLE IV. Spectroscopic data from inelastic scattering of 15-MeV deuterons from Ni^{60}. See also the caption for Table II.

Excitation energy (MeV) Present work	Ref. 16	Ref. 20	$\frac{d\sigma}{d\Omega}(46°)_{c.m.}$ (mb/sr)	J^π Present work	Ref. 16	Ref. 21	$\frac{B(El;0\to l)}{B_{s.p.}(El;0\to l)}$ Present work	Elsewhere	β_l
1.33	1.333		3.29	2^+	2^+		27	{13 (Ref. 14) 17±2 (Ref. 22)	0.30
2.16	2.159		0.11		$2^{(+)}$				
2.29	2.285		0.050		(0^+)				
2.51	2.504		0.43		4^+				
2.63	2.624		~0.02			3^+			
3.13	3.120		0.16	3^-	$2^{(+)}$		3		0.09
3.31	3.316		0.09	(2^+)			0.9		0.05
3.38	3.391		0.025						
3.70	3.732	3.670	0.12						
3.91	3.92	3.886	0.048						
4.05	4.038		0.55	3^-			12	16±2.5 (Ref. 21)	0.19
4.35		4.322	0.14						
4.53			0.06	(3^-)			1.3		0.06
4.63			0.07						
4.85			0.024						
5.02		5.1	0.08						
5.14			~0.1						
5.26			0.25	(2^+)			3.5		0.10
5.46			0.13(?)						
5.68		5.7	0.22(?)						
5.82			0.09						
5.95			0.10						
6.18	6.2		0.12						

(except for the cases of $l=0$), have been made with calculations including Coulomb-excitation effects. Detailed results of such analyses in individual nuclei are discussed below.

1. $Sn^{120}(d,d')$

Most deuteron groups observed in the inelastic deuteron spectra from Sn^{120} seem to be well resolved. Some of the data from these measurements are presented in Figs. 8, 9, and 10—where the experimental points are compared with DWBA predictions—and listed in Table II. These data were measured using magnetic analysis of the various inelastic deuteron groups and show heavy deuteron background from slit scattering at angles less than 40°. Consequently, except for the case of the most intense deuteron groups,

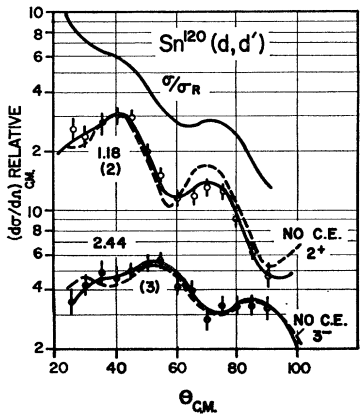

FIG. 8. Angular distributions of the elastic and the inelastic groups leading to the strongly excited 2^+ and 3^- states in Sn^{120}. The elastic curve is simply a smooth graph drawn through the experimental points. The curves through the data points for the 2^+ and 3^- states are DWBA calculations both with (solid curve) and without (broken curve) the contribution from Coulomb excitation. The numbers on the left are excitation energies and the angular momentum transfer (within parentheses) in the inelastic collision.

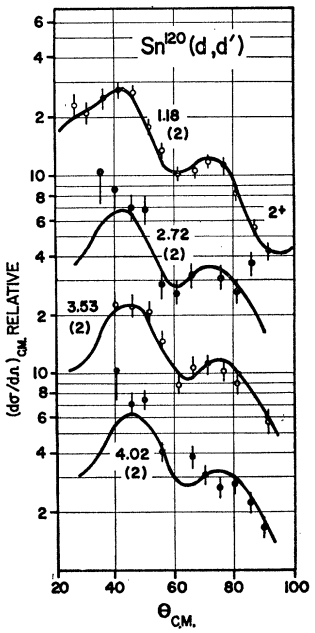

FIG. 9. Angular distributions of the inelastic deuteron groups leading to the 1.18-, 2.72-, 3.53-, and 4.02-MeV states in Sn^{120}. The solid curves going through the data points are the DWBA predictions for quadrupole single excitations at the corresponding excitation energies. See also the caption for Fig. 8.

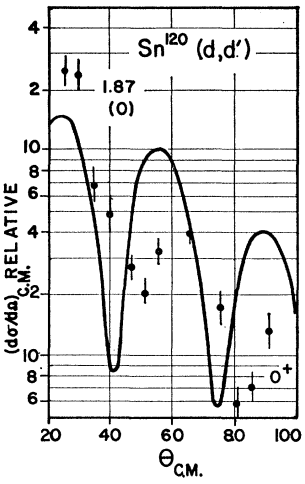

FIG. 10. Angular distribution for the 1.87-MeV 0^+ state in Sn^{120}. The curve is the DWBA prediction for monopole excitation at 1.87 MeV without the contribution from Coulomb excitation, as explained in the text.

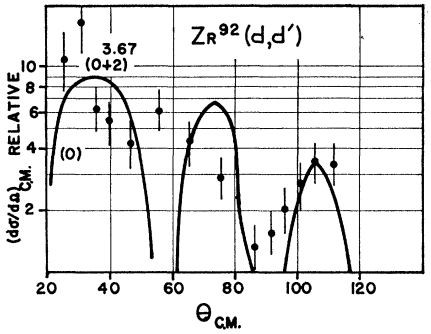

FIG. 12. Angular distribution of the 3.67-MeV group in the spectrum of Zr^{92} (d,d'). The curve is the DWBA prediction for a monopole excitation without the contribution from Coulomb excitation, as explained in the text.

the experimental points for these angles have large uncertainties. One feature which is peculiar to these data is the dominance of a group of levels above 2.4 MeV of excitation energy whose angular distributions agree quite well with the theoretical single-excitation curves for $l=2$. Details of spectroscopic analyses of the various groups observed in these spectra are presented below.

The most intense deuteron groups in $Sn^{120}(d,d')$ spectra are observed at 1.18 and 2.44 MeV. The former is known to come from the first excited quadrupole oscillation, while the latter can be seen from energy systematics for neighboring nuclei,[1] and from cross-section information, to represent the strongly excited octupole oscillation. The agreement between the experimental angular distributions and the DWBA predictions (including Coulomb-excitation effects) is very good (Fig. 8). The reduced transition strength (Table II), in terms of single-particle estimates, for the 1.18-MeV state is known from Ref. 14 and agrees fairly well with the value found in this work. It may be remarked here that the improvement of agreement between theory and experiment by the inclusion of Coulomb-excitation effects is very strikingly demonstrated in Fig. 8.

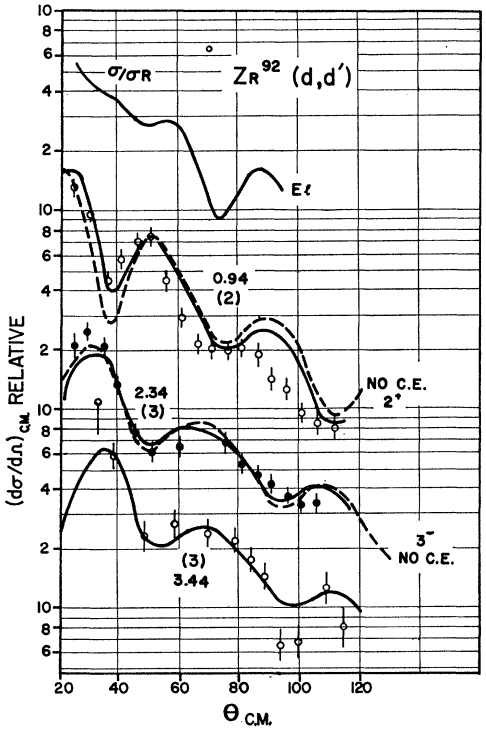

FIG. 11. Angular distributions of the elastic and inelastic groups leading to the strongly excited 2^+ and 3^- states and also a level at 3.44 MeV in Zr^{92}. See also the caption for Fig. 8.

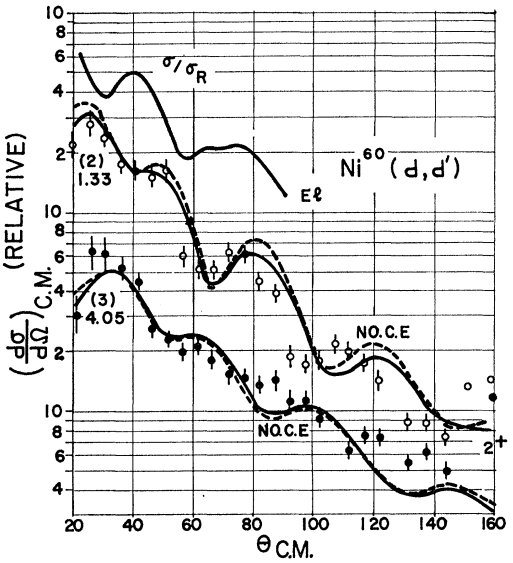

FIG. 13. Angular distributions of the elastic and inelastic groups leading to the strongly excited 2^+ and 3^- states in Ni^{60}. See also the caption for Fig. 8.

[14] L. S. Kisslinger and R. A. Sorensen, Rev. Mod. Phys. **35**, 853 (1963).

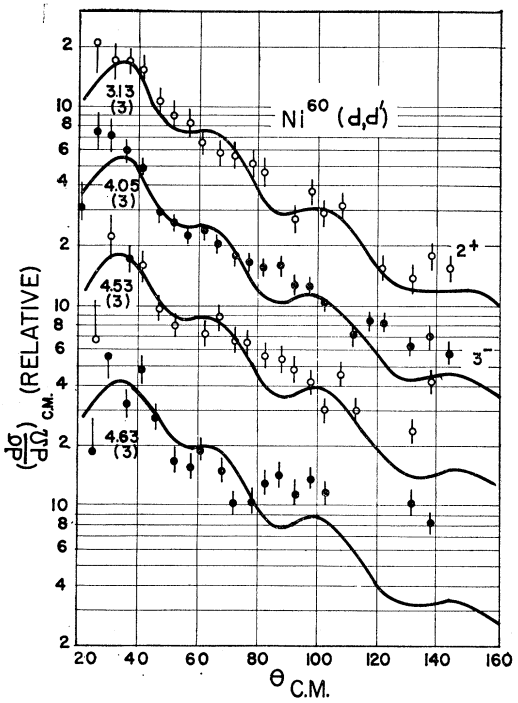

FIG. 14. Angular distributions of inelastic groups leading to the 3.13-, 4.05-, 4.53-, and 4.63-MeV states in Ni^{60}. The solid curves going through the data points are the DWBA predictions for single octupole excitations. See also the caption for Fig. 8.

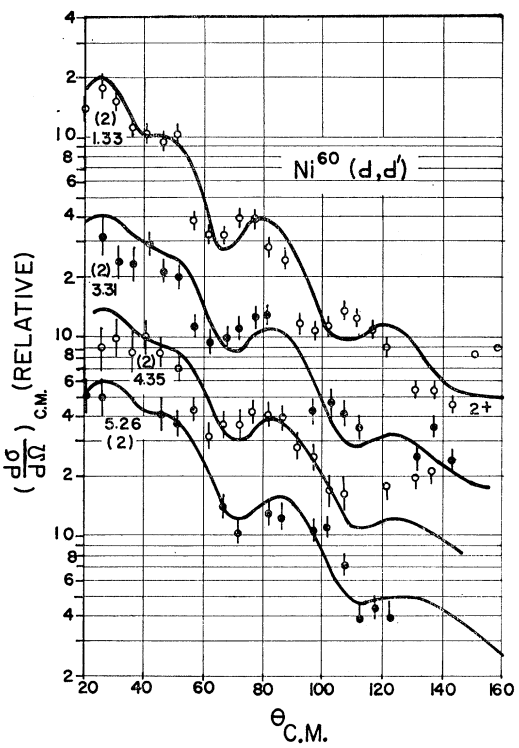

FIG. 15. Angular distributions of the inelastic deuteron groups leading to the 1.33-, 3.31-, 4.35-, and 5.26-MeV states in Ni^{60}. The data have been compared with the DWBA predictions for $l=2$. See also the caption for Fig. 8.

Two 0^+ states which are known from previous work (see Table II) have also been observed in these analyses. Their excitation energies are 1.87 and 2.63 MeV. The angular distribution for the former is quite certain and has been presented in Fig. 10. For the latter the uncertainties in cross sections are quite large, although the over-all trend of the experimental points does indicate an angular-momentum transfer $l=0$. The disagreement between the theoretical prediction and the experimental data in Fig. 10 should not be very disturbing on account of the uncertainties in $l=0$ transition calculations mentioned above.

As stated above, beyond 2.4 MeV of excitation energy there are several groups whose angular distributions agree with the DWBA prediction for an $l=2$ single excitation. In addition to the 1.18-MeV group discussed above, others that belong to this category are the groups at 2.11, 2.72, 2.89, 2.99, 3.12, 3.21, 3.32, 3.44, 3.53, 3.74, 3.82, 4.02, and 4.10 MeV of excitation energy. Of the groups listed above, the agreement between the theoretical curves and the experimental data for those at 2.72, 3.53, and 4.02 MeV (Fig. 9) is a little more than accidental. Consequently, the reduced transition strengths and β_l's for these states based on the spin and parity assignment (2^+) have been listed in Table II. Some of the weakly excited states between 3.2 and 3.8 MeV may belong to the quadrupole-octupole two-phonon multiplet for which some evidence has been seen in the analyses of $Cd^{114}(p,p')$ data by Sakai and Tamura.[15]

The experimental angular distributions for the 2.23- and 2.31-MeV groups (Table II)[16,17] are quite alike, but different from the DWBA predictions for any reasonable value of angular momentum transfer. As we shall see below in the case of the other two nuclei, there are indications here of the possibility that these states are members of the quadrupole two-phonon triplet. This conclusion also derives support from the fact that their excitation energies are about twice that of the first excited 2^+ state. Coupled-channel analyses of the data for these and analogous states in Ni^{60} and Zr^{92} nuclei by Tamura of Oakridge National Laboratory are currently in progress, and it is only after the completion of these analyses that we shall be more certain of their two-phonon nature. The angular distributions of the rest of the groups listed in Table II are very ambiguous, either on account of our inability to resolve neighboring groups very clearly or on account of uncertainties in experimental cross sections. Of these, however, the 4.17-MeV group has an angular distribu-

[15] M. Sakai and T. Tamura, Phys. Letters **10**, 323 (1964).
[16] *Nuclear Data Sheets*, compiled by K. Way *et al.* (Printing and Publishing Office, National Academy of Sciences—National Research Council, Washington 25, D. C. 1963), NRC 60-04-66 and 60-05-80.
[17] S. Yoshida, Nucl. Phys. **38**, 380 (1962).

tion that has indications of an angular-momentum transfer $l=0$. Similarly the angular distributions for the 3.67-, 3.90-, 4.28-, 4.36-, 4.44-, and 4.60-MeV groups have some resemblance to an $l=2$ theoretical curve.

2. $Zr^{92}(d,d')$

The experimental angular distributions for most deuteron groups and their comparison with DWBA predictions are shown in Figs. 11 and 12, and the results of spectroscopic analyses are listed in Table III.[18,19]

In Fig. 11 the experimental angular distributions for the 0.94- and 2.34-MeV groups have been compared with the DWBA predictions including (solid curve) and excluding (dashed curve) Coulomb excitation. There is some evidence in the case of the 0.94-MeV group that the agreemet between theory and experiment is improved by including Coulomb-excitation effects in the DWBA calculations; the change in the theoretical angular distribution for the 2.34-MeV group is not large enough to commend one calculation over the other. The 0.94- and the 2.34-MeV states were previously known to be the most strongly excited 2^+ and 3^- levels of Zr^{92}. While agreement between theory and experiment is quite good for the 2.34-MeV group, there are some differences between the theoretical and experimental angular distributions for the 0.94-MeV group. The "peak-to-valley" ratio is the same as in the experimental angular distribution but the maxima and minima in the experimental angular distribution appear at progressively smaller angles relative to the theoretical (solid) curve. The reduced transition rate for the strong quadrupole oscillation is known from previous Coulomb excitation work (see Table III) and agrees reasonably well with our result (calculated in an angular region where theory and experiment agree).

The next known states in the level spectrum of Zr^{92} are the 0^+, 4^+, and 2^+ at 1.38, 1.49, and 1.84 MeV of excitation energy. The data for the 1.84-MeV group seem to be out of phase with the experimental angular distribution for the 0.94-MeV group. Similarly the data for the 1.49-MeV group somewhat disagree with the DWBA calculation for $l=4$ in that the experimental angular distribution has a greater peak-to-valley ratio and maxima (minima) located at smaller angles than in the theoretical curve. Another interesting feature of the experimental angular distributions for the 1.49- and 1.84-MeV groups is the general similarity in their shapes. This feature has been previously noted for the quadrupole two-phonon states in the data for Sn^{120} and has also been seen more strikingly in the data for Ni^{60}. So most probably these are the members of the quadrupole-oscillation two-phonon triplet. This observation is further supported by the facts that (1) these groups occur at approximately twice the excitation energy of the 2^+ first excited state and (2) there is marked disagreement between the experimental angular distributions and the theoretical curves which have been calculated for single excitations.

The 1.38- and 3.67-MeV states lead to angular distributions whose most prominent feature is the large-amplitude oscillations that are typical of $l=0$ transitions. The theoretical angular distribution (excluding Coulomb excitation effects) for $l=0$ does not agree with the data, as is expected from the example of the 1.87-MeV 0^+ state in Sn^{120} (Fig. 10), although the difference in the present case is seen to be a little more striking than in the case of Sn^{120}. The latter fact may be due to the 1.38-MeV level's being a member of the quadrupole-oscillation two-phonon triplet. This idea also derives support from the fact that the angular distribution of the 3.67-MeV group (Fig. 12) is out of phase with the angular distribution of the 1.38-MeV group at large angles. The agreement of the 3.67-MeV-state data with theory is better in that the two angular distributions somewhat agree in the location of their "valleys" (Fig. 12). The reduced transition rates for the groups discussed above have not been calculated, since the differential cross sections for $l=0$ transitions are inaccurate because of the uncertainties referred to above.

The angular distributions of the 2.75-, 3.25-, 3.44-, and 3.90-MeV groups are alike in that they all seem to belong either to $l=3$ or to $l=4$ transitions. The experimental angular distribution for the 3.44-MeV group (Fig. 11) strongly favors a 3^- assignment. In the other three cases the assignments are more ambiguous, though there is some preference for a 4^+ assignment for the 2.75- and 3.90-MeV groups. There is a possibility that some of these states are members of the quadrupole-octupole two-phonon multiplet, since these groups appear at the appropriate energy for such a multiplet.

The angular distributions of the other groups listed in Table III are very uncertain, on account of either low resolution or poor statistical accuracy. But very crude indications from the gross features of the angular distributions are discussed below. The 2.04-MeV group seems to be a mixture of $l=2$ and 3 or 4 transitions. The 2.48-MeV group has very large uncertainties in cross sections, particularly at forward angles; $l=3$ or 4 seem to be good possibilities. The 2.85-MeV group is not resolved from the 2.75-MeV group at most angles. The data show features of an $l=3$ or 4 transition. The differential cross sections for the 4.46-MeV group are very uncertain, though the possibility of an $l=3$ or 4 transition is definitely there. The 4.81-MeV group has a completely undecipherable angular distribution, while the angular distribution for the 5.51-MeV group indicates an $l=4$ or 5 transition.

[18] B. L. Cohen and O. V. Chubinsky, Phys. Rev. **131**, 2184 (1963).
[19] D. S. Andreyev, A. P. Grinberg, K. I. Erokhina, and I. Lenberg, Nucl. Phys. **19**, 400 (1960).

3. $Ni^{60}(d,d')$

The data and calculations for Ni^{60} are shown in Figs. 13, 14, and 15 and listed in Table IV.[20–22] By far the most strongly excited levels in these studies are the 1.33-MeV 2^+ and the 4.05-MeV 3^- single-phonon excitations. The angular distributions for both of these states are compared with DWBA predictions for $l=2$ and $l=3$ transitions, both with and without Coulomb-excitation effects (Fig. 13). Once again it can be seen that inclusion of Coulomb-excitation effects in the DWBA calculations improves the agreement between theory and experiment noticeably (as in the case of the 1.33-MeV group). The experimental angular distribution for the 1.33-MeV group agrees with theory (solid curve) up to 50°, beyond which the maxima and minima in the experimental differential cross section occur at progressively smaller angles as compared to the theoretical cross section. This is the same observation as noted above in the case of Zr^{92}. One also notices a rise in the differential cross sections towards very large angles (greater than 140°). In the case of the 4.05-MeV group, the experimental data agree with theory up to 60°. At angles greater than 60°, the experimental angular distribution shows practically no oscillations and also shows a rise in cross section at very large angles. However, it may be noticed in Fig. 13 that the over-all agreement between theory and experiment is good enough to enable a distinction between $l=2$ and $l=3$ transitions to be made. The reduced transition strengths for both of these states are already known from electron scattering and Coulomb-excitation work and are compared with our results in Table IV. The agreement is qualitatively good, taking into account the aforesaid differences between theory and experiment compounded with the uncertainties in experimental cross sections. The angular distributions of the 3.31-, 4.35-, and 5.26-MeV groups (Fig. 14) agree in shape with the DWBA calculations for an angular-momentum transfer of 2 units. The assignment of spin and parity of 2^+ for the 3.31-MeV state is quite certain. The 4.35-MeV group is an unresolved doublet of states that are ~50 keV apart. Evidence for this is derived from an examination of the width of the 4.35-MeV group and from the observation that at some angles this group is resolved into two groups with the separation mentioned above. The intensities of both groups were added wherever necessary to get the angular distribution of the 4.35-MeV group. The more intense of the two groups at 4.35 MeV is probably from a 2^+ state, while the weaker could be from a 3^- or 2^+ state. It may however be kept in mind that $Ni^{60}(d,d')$ data in this region of excitation energy show several 3^- states, as we shall see below. The 5.26-MeV group is seen to be among several closely spaced groups between 4.9 and 5.3 MeV, but it is the most intense of them all. Its angular distribution strongly resembles that of an $l=2$ transition, so that the 5.26 MeV state is probably of spin and parity 2^+.

Another interesting group of states is the 0^+, 2^+, and 4^+ triplet occurring at 2.29, 2.16, and 2.51 MeV of excitation energy, respectively. The angular distributions of the 2.16- and 2.51-MeV groups look almost exactly alike. This is a typical feature of the angular distributions for the 2^+ and 4^+ members of the two-phonon quadrupole-oscillation triplet, as noted in the cases of the other two nuclei. Some preliminary angular-distribution measurements in $Ni^{62}(d,d')$ showed exactly similar results for the analogous states in Ni^{62}. The angular distributions of the 2.16- and 2.51-MeV groups seem to be somewhat in phase with that for the 4.05-MeV 3^- group, but the data do not agree (in the sense described above for the 4.05- and 1.33-MeV groups) with any of the theoretical predictions, which supports the conclusion that these two states are members of the two-phonon triplet. They also show a rise in cross sections at backward angles. The shape of the angular distribution for the 0^+, 2.29-MeV state is somewhat in agreement with the theoretical prediction without the Coulomb-excitation contribution.

The other angular distributions shown in Fig. 15 are for the groups at 3.13, 4.53, and 4.63 MeV. All of these agree with the theoretical prediction for an $l=3$ transition, though the large uncertainty in the cross sections for the 4.63-MeV group makes the assignment 3^- a little doubtful. The angular distribution of the 3.13-MeV group is most interesting, as the data almost certainly show an $l=3$ transition. Matsuda[23] has presented a diagram of energy systematics of a second 3^- which he has noticed in several nuclei from O^{16} to Zn^{64}. We reproduce his diagram here (Fig. 16) with our 3.13-MeV level shown cross-hatched in the spectrum

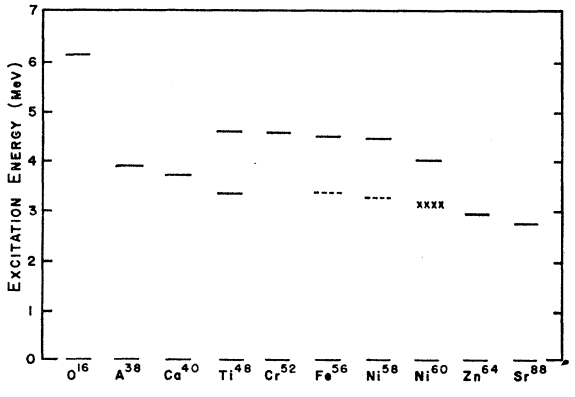

FIG. 16. A diagram showing the energy systematics of the 3^- states observed in the nuclei from O^{16} to Sr^{88}. The 3.13-MeV state in Ni^{60} observed in this work is shown by a row of X's in the figure. Other results were compiled by Matsuda (Ref. 23).

[20] H. W. Broek, Phys. Rev. **130**, 1914 (1963).
[21] D. M. Van Patter and R. K. Mohindra, Phys. Letters **12**, 223 (1964).
[22] H. Crannel, R. Helm, H. Kendall, J. Oeser, and M. Yearian, Phys. Rev. **123**, 923 (1961).
[23] K. Matsuda, Nucl. Phys. **33**, 536 (1962).

of Ni^{60}. The analogous levels in the neighboring nuclei (shown by broken lines) have been reported by Matsuda[23] and Satchler *et al.*[24] This indicates that the 3.13-MeV state is of spin and parity 3^-. However, from the analyses of the β^+ decay of the 24-min 2^+ ground state of Cu^{60} by Levine and Naussbaum *et al.*[25] and of $Ni^{60}(p,p'\gamma)$ data by Van Patter *et al.*,[22] the level in question seems to be of spin and parity 2^+. There is also some evidence from analyses of $Ni^{61}(d,t)$ data by Fulmer *et al.*[8] supporting the 2^+ assignment. The fact that β^+ decay and (d,t) assignments agree in this case is not surprising, since both interactions probably involve rather simple final-state configurations. [This argument can be applied even to (p,p',γ) data to a certain extent.] But it is not very surprising if the same states are not appreciably excited in inelastic scattering of 15-MeV deuterons. There is some evidence in favor of the latter statement in the case of the 2.42-MeV state in Sn^{120}, which is well known to be the strongly excited octupole oscillation (3^-) when it is excited by inelastic scattering,[2] but is believed to be a 6^+ state when it comes from β^+ decay of Sb^{120}.[16] It is, therefore, quite probable that different states are being excited in inelastic deuteron scattering and the experiments mentioned above, since the evidence in support of a 3^- assignment in the present work is a little more than circumstantial. The problem encountered above is, however, very interesting and needs to be investigated further.

The angular distribution of the 3.91-MeV group at forward angles (where theory and experiment are very similar) agrees quite well with the curve for an $l=3$ transition. The situation is not so clear in the case of the 3.70-MeV group. There is a low background in $Ni^{60}(d,d')$ spectra at angles between 80 and 100 deg which has not been subtracted because of uncertainty about its magnitude, so that in the angular distributions of low-intensity groups (see Table IV) the data in this angular range may be too high. Keeping this correction in mind, there may be a preference for a 3^- assignment for the 3.91-MeV level, though the situation is far from definite. The 3.70-MeV group is a close doublet which is seen resolved into 3.65- and 3.75-MeV groups at several angles. Assuming that the two groups have similar angular distributions, the angular distribution for the sum of their intensites resembles the theoretical curves for either $l=3$ or 4 single-excitation transitions. The cross sections for these states (Table IV) are comparable to those of the two-phonon states, so it is very unlikely that these are members of the quadrupole three-phonon quintet. (The cross sections for the three-phonon states should be at least an order of magnitude smaller than the two-phonon-state cross sections.) The situation for the 5.46-MeV group seems similar to that for the 3.91-MeV group, while the 5.95-MeV group shows some preference for a 3^- assignment.

The angular distributions of the remaininig groups listed in Table IV have not been analyzed because of large uncertainties in their data. However, the following remarks may be made about the possible spins and parities suggested by the trends in their angular distributions.

Of these, the case of the *unnatural-parity* 2.63-MeV state is very interesting. This state is believed to be of spin and parity 3^+ from the work of Van Patter *et al.*[21] In the $Ni^{60}(d,d')$ energy spectra it has the lowest cross section and is barely distinguished from the background at most angles. Consequently, no reliable angular distribution could be obtained from the data on this state. But the observation in the case of this state—viz., that an unnatural-parity state is excited with an extremely low cross section in (d,d')—, if generally true, is good evidence in support of the collective model of single excitations observed in inelastic deuteron scattering, where spin and parity are determined soley by the orbital-angular-momentum transfer in the inelastic collision. The assertion of Van Patter *et al.* that this is the lowest 3^+ member of a three-phonon quintet ($0^+,2^+,3^+,4^+,6^+$) is also tenable, since one does expect the cross sections for the members of the three-phonon quintet to be extremely small.

The cross sections for the 3.38-MeV state are practically the same as those of the 2.63-MeV state discussed above, so that no information could be extracted from the angular distribution for this state.

The cross sections for the 4.85- and 5.68-MeV groups are very uncertain at most angles, so that no meaningful indications can be obtained from their angular distributions. The data for the 5.02- and 5.14-MeV groups are very indefinite at small angles, though there are some indications for $l=3$ or 4 transitions leading to these groups. The angular distributions of the 5.82- and 6.18-MeV groups are quite similar in their gross features. The 6.18-MeV group is not very well resolved from another possible group at 6.3 MeV and seems to have large-amplitude oscillations as compared to the 5.82-group. The latter group, however, has indications of an $l=3$ or 4 transition. There are also some indications from previous work[20] for the 6.18-MeV level to be of spin and parity 3^-.

The results of the analyses in this work have been summarized in Fig. 17, where spectroscopic data on the energy levels of Sn^{120}, Zr^{92}, and Ni^{60} have been compared with those from other sources (see Tables II, III, and IV).

C. Status of the Blair's Phase Rule

The data presented above afford a very good opportunity to re-examine the phase rule for inelastic scattering of 15-MeV deuterons in some detail. The angular distributions of the elastic and the most intense 2^+ and 3^- groups have been compared in Figs. 8, 11,

[24] G. R. Satchler, R. H. Bassel, and R. M. Drisko, Phys. Letters **5**, 256 (1963).

[25] N. Levine, H. Frauenfelder, and A. Rossi, Z. Physik **151**, 241 (1958); also R. H. Nussbaum, R. Van Lieshout, A. H. Wapstra, N. F. Werster, F. E. L. Ten, G. J. Nijgh, and L. T. M. Ornstein, Physica **20**, 555 (1954).

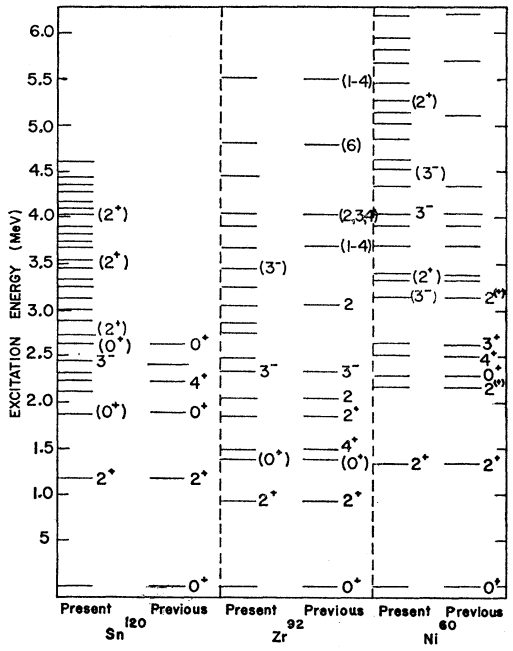

FIG. 17. A diagram comparing the levels observed in the present work with those known from other sources (see Tables II, III, and IV).

and 13. The observations in the various cases discussed above are summarized below.

(1) The phase rule is quite successful in predicting the relative phases of the oscillations in the angular distributions for the 2^+ and 3^- states.

(2) With the exception of Ni, the phase rule completely breaks down with regard to the angular distributions of the elastic group as compared with those for the inelastic groups that lead to the 2^+ and 3^- states.

(3) The angular distributions for the two-phonon, 2^+ and 4^+ states tend to be in phase with those for the 3^- states but the relationship is not as clear as in the case of the 2^+ states.

(4) The phase rule does not seem to apply to the angular distributions for the 0^+ states.

Thus, it seems that the phase rule is of limited use in inelastic scattering of 15-MeV deuterons from nuclei.

V. CONCLUSIONS

The important conclusions from the analyses discussed above are as follows:

(1) DWBA calculations (based on a deformed optical-model potential) of inelastic deuteron-scattering differential cross sections, using optical-model parameters obtained from a best fit to the elastic-scattering data, can be reliably used for spectroscopic analyses of single excitations. But Blair's phase rule is best used only for intercomparisons of angular distributions for the octupole and quadrupole excitations.

(2) Inclusion of Coulomb excitation effects in DWBA calculations improves the agreement between theory and experiment.

(3) Use of complex coupling is essential for correct single-excitation calculations in inelastic scattering of 15-MeV deuterons from intermediate-mass nuclei.

(4) The experimental angular distributions for the 2^+ and 4^+ members of the two-phonon triplet have very similar gross features, so that measurement of angular distributions in inelastic scattering of 15-MeV deuterons does not seem to be a good tool for spin and parity assignments to these members of the two-phonon triplet. The differences may become more obvious at higher energies.

ACKNOWLEDGMENTS

The author owes his sincerest thanks and appreciation to Professor B. L. Cohen for suggesting this problem and for his constant guidance throughout this work. The author is especially indebted to Professor R. M. Drisko for his invaluable help in doing the DWBA calculations and many stimulating discussions and useful suggestions. He also wishes to thank Professor W. W. Daehnick for the use of his equipment and his constant help in setting it up. The help of R. H. Fulmer and the technical staff of the cyclotron in taking data and that of Addie Trent and co-workers in plotting the data is sincerely appreciated. The assistance and support of the Tandem Van de Graaff Accelerator Program of the Florida State University (supported by the U. S. Air Force Office of Scientific Research) in preparing the final manuscript is gratefully acknowledged. The author is also very thankful to Dr. J. B. Ball of the Oak Ridge National Laboratory for lending him a Zr^{92} target.

The calculations reported in this article were performed at the University of Pittsburgh computation center which is partially supported by the National Science Foundation under Grant No. G-11309.